



Citation for published version:

Storey, JP, Wilson, PR & Bagnall, D 2013, 'Improved Optimization Strategy for Irradiance Equalization in Dynamic Photovoltaic Arrays', IEEE Transactions on Power Electronics, vol. 28, no. 6, pp. 2946-2956.
<https://doi.org/10.1109/TPEL.2012.2221481>

DOI:

[10.1109/TPEL.2012.2221481](https://doi.org/10.1109/TPEL.2012.2221481)

Publication date:

2013

Document Version

Early version, also known as pre-print

[Link to publication](#)

© 2013 IEEE. Personal use of this material is permitted. Permission from IEEE must be obtained for all other users, including reprinting/ republishing this material for advertising or promotional purposes, creating new collective works for resale or redistribution to servers or lists, or reuse of any copyrighted components of this work in other works.

University of Bath

General rights

Copyright and moral rights for the publications made accessible in the public portal are retained by the authors and/or other copyright owners and it is a condition of accessing publications that users recognise and abide by the legal requirements associated with these rights.

Take down policy

If you believe that this document breaches copyright please contact us providing details, and we will remove access to the work immediately and investigate your claim.

Improved Optimization strategy for Irradiance Equalization in Dynamic Photovoltaic Arrays

Jonathan Storey, Peter Wilson, *Senior Member, IEEE*, Darren Bagnall

Abstract—This paper proposes an improved strategy for the optimization of dynamic photovoltaic arrays (DPVA) utilizing the ‘irradiance equalization’ reconfiguration strategy. This type of reconfigurable array is already very robust as it amalgamates the flexibility of dynamic reconfiguration with the averaging ability of Total Cross Tied (TCT) array architecture. This paper identifies four areas to further increase the power yield and significantly reduce the time for a return on investment. Results indicate potential efficiency improvements of more than 10% in some cases, and between 4-10% across a number of random and abrupt shading conditions. As in any DPVA system the proposed approaches require additional hardware and advanced control algorithms compared to a static PV array, but anyone implementing a dynamic array has already committed themselves to including the majority of this infrastructure. This investigation supports the idea of a fully dynamic IEq-DPVA with the ability to resize its array dimensions while implementing a rapid sorting algorithm based on information gathered using a novel precision irradiance profiling technique.

Index Terms— Dynamic Photovoltaic Array, Reconfigurable, Irradiance profiling

I. INTRODUCTION

The field of Photovoltaic (PV) energy production is one of the most researched and industrially influential energy subjects in the last few decades. Between 1983 and 2008 the power produced by a single crystalline solar cell increased by 57% [1], and the recent boom in the PV market saw the industry grow by 139% in 2010 alone[2]. As the basic cell efficiency increases and corresponding overhead production cost reduces, the global interest in PV power will continue to expand for many years to come. Despite these advances, fundamental limitations of current PV cell technology mean that efficiencies of more than 31% are realistically unattainable, with many commercially available modules closer to 20% efficiency. Schockley and Quisser [3] demonstrated in their classic paper that incomplete absorption due to the band gap would limit the maximum theoretical efficiency of a single junction cell to 44%. Further losses including optical limitations and reflections mean that in practice this would be even further reduced as illustrated by Bagnall and Boden [4]. This limit means that optimization of a

PV installation by relatively minor amounts can significantly increase the overall effectiveness of the system and reduce its return on investment (ROI) time significantly. Numerous fundamental techniques have been investigated to improve the ability of cells and materials to convert light energy into electricity including plasmonics, thin film and multi-junction devices, all of which are beyond the scope of this paper. While these efforts have seen the physical devices become better at converting the incident solar irradiance into DC electricity, the fundamental limitations remain.

In this work, we have operated on the principle that whichever technology is used, environmental and installation optimization are crucial to maximizing the benefit of the array. Most PV arrays are destined to be installed once and then remain *in situ* and face an unpredictably chaotic irradiance environment for at least 25 years. During this time, the environment can range from uniform direct beam, uniform defused hue or a non-uniform combination of the two. Issues with ‘non uniform irradiance’ are compounded when trying integrating PV into buildings (BiPV) or vehicles as these frames tend to have curved contours that do not always directly face the sun.

Solar cells produce a current that is proportional to the irradiance that falls on its surface using the fundamental mechanism described by Einstein [5] and this is often idealized to be the short circuit current (I_{SC}). It is possible to force more current than this through a cell but it will be operating under reverse bias and quickly begin consuming power and this will result in significant thermal losses. Because of this rapid change from producer to consumer when I_{SC} is exceeded, strings of solar cells are subject to the ‘weakest link’ condition where the maximum possible current is nearly equal to the I_{SC} of the weakest cell in the string.

Almost all modern PV modules are equipped with bypass diodes internally connected across the strings of solar devices. These diodes allow the module to safely tolerate partial shading conditions and still produce a current in excess of I_{SC} of the weakest cells. A bypass diode that is in operation will cause a number of cells to produce no power, it also introduces a voltage drop from power that is produced and they cause situations which can confuse an MPPT into operating sub-optimally. They are considered essential for the safety and performance of the array but they also introduce potential losses. A few interesting methods for reducing the side effects include ‘cold bypass switching’ (CBS), ‘Active voltage sharing’ and ‘Returned Energy Current Converters’ (RECCs) [6-8] respectively.

A recent approach to alleviate the issues caused by bypass

Manuscript received May 15th, 2012

J. Storey, P Wilson and D Bagnall are with the School of Electronics and Computer Science, University of Southampton, Southampton UK; Email:

J. Storey, P Wilson and D Bagnall are with the School of Electronics and Computer Science, University of Southampton, Southampton UK; Email: prw@ecs.soton.ac.uk.

diodes while maintaining their ability to permit partial shading involves dynamically reconfiguring the electrical connections of cells within and array. The introduction of dynamically altered arrays begins as far back as 1990 where the configuration of a solar array was altered in order to change the IV characteristic presented to a load. These types of systems are limited in complexity and focused on optimizing power extraction under a falling but uniform distribution of irradiance. This class of DPVA is referred to as a fixed configuration dynamic photovoltaic array (FC-DPVA) [9-11].

More modern DPVAs are specifically designed to mitigate issues with significant partial shading (as expected within urban environments). Two main classes of DPVA seem to have been developed and each has smaller sub categories within them. ‘Irradiance Equalized’ DPVAs (IEq-DPVA) are the focus of this paper and their primary attribute is they rely on the averaging characteristic of a TCT structure to mitigate issues [12-16]. There are various other publications on a class referred to as ‘String Configured’ DPVA (SC-DPVAs) and they rely on forming sets of strings that do not include failing cells. [17-20]. It should be noted that if an array is to be situated in a location where partial shading is rare, a normal bypassed array would be more suitable.

It is also important to note that whatever reconfiguration technique is ultimately applied there will be some form of MPPT connected to the system. *Jiet al* in [24] discusses how the use of MPPT in an intelligent manner can compensate for partial shading conditions to a certain extent. More generally, there have been a number of recent developments in MPPT optimization, including adaptive perturbation and swarm optimization techniques [25-29] which mitigate some of the problems in sub-optimal conditions.

Despite all these advances, the fundamental limitation in practical PV systems remains that the power output is ultimately constrained by the physical connections of the network of modules or cells, and we will show in this paper precisely how this can be quantified. Our proposed system works on the principle that if the modules can be connected in an arbitrary manner, then ultimately an increase of power will be the result. The concept of a dynamic array in itself is not new. As will be discussed in more detail in the next section of this paper, the use of techniques such as Irradiance Equalization [12] allow the module to be configured in ways to improve the power output, however a serious practical issue still remains of the method by which the optimal power output can be obtained. The ~~possible~~ number of possible configurations can be astronomical for more than the very simplest array sizes, and so most search algorithms will either be computationally expensive (if tractable at all) or will take such a long time that responding quickly enough to relatively fast changes in irradiance in a congested urban environment in particular will be impossible. This paper proposes a very simple sort algorithm that can be applied to existing arbitrary sized array architectures and provides an optimum solution in a very fast time, with even the most basic processing unit such as a simple 8 bit microcontroller. The results of the different configurations were obtained using a standard simulation platform where each different configuration was evaluated using identical models for the individual cells and modules,

and at each stage the maximum power was calculated making the assumption that regardless of the configuration of the array, perfect maximum power point tracking was in place. In all the examples used in this paper an array of 16 identical modules is used. This array of modules can be configured in any form in terms of rows and columns, where the only limitation is the maximum number of rows. This is defined by the number of individual bus bars specified by the system designer, and in this example case given in this work, the array can range from a default grid of 4x4 to any other variation as long as the number of rows does not exceed 4. The voltage will obviously change depending on the number of cells in series, and so the assumption is made that the power electronics can cope with a wide range of array voltages. Of course, in practice there will be constraints, and these could be taken into account in limiting the possible range of cells in individual columns (for example the minimum number of rows could be 3 and the maximum could be 6).

The remainder of this paper is structured as follows. Section II will introduce some typical static array types, to provide the baseline performance to which the other dynamic arrays can be compared. Section III discusses the general approach of Irradiance Equalization, Section IV discusses optimizing the IEq-DPVA, Section V summarizes the key results and Section VI provides a conclusion.

II. REFERENCE STATIC PV ARRAYS

A. Introduction

In order to provide a reference point for the more complex dynamic arrays, and also to demonstrate the impact of shading very clearly, it is useful to observe the behavior of standard PV array structures under different types of shaded conditions. Given a nominal test array size of 4x4 (16 modules) in total, we have created a reference cell model based on the standard circuit level as shown in Figure 1 and described by equation (1).

$$i = i_{sat} * \left(e^{\frac{qV}{nkT}} - 1 \right) - \frac{V}{R_{shunt}} \quad (1)$$

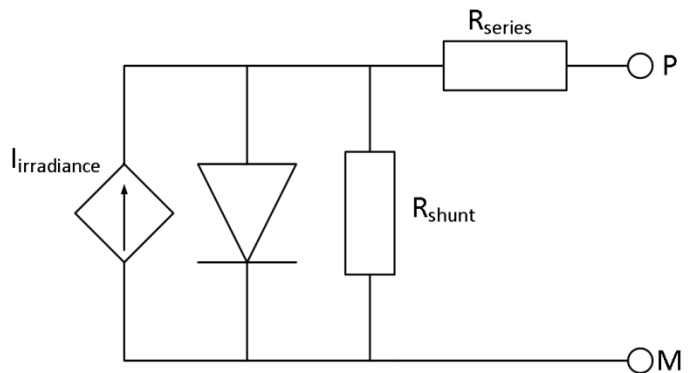


Figure 1: Standard Circuit Level PV Cell Model

This model allows the system to be tested across the complete voltage and current range and obtain the correct maximum power while setting the correct irradiance on every

individual cell in the array. The resulting behavior is the classic PV cell current and power curve, where the maximum power can be measured on the power curve as the voltage is swept from the short circuit condition ($V=0$) to the open circuit case ($V=V_{oc}$). Using values which represent a reasonably typical 80W panel, we can see the behavior under 1 sun conditions ($1000W/m^2$) giving a maximum power of 80W in Figure 2.

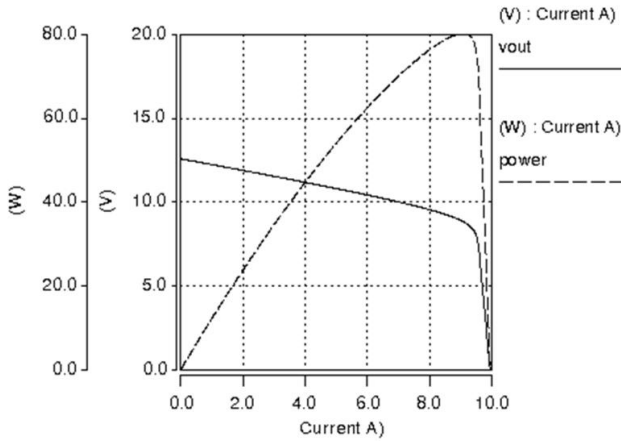


Figure 2: Model of 80W nominal panel Current and Power vs.

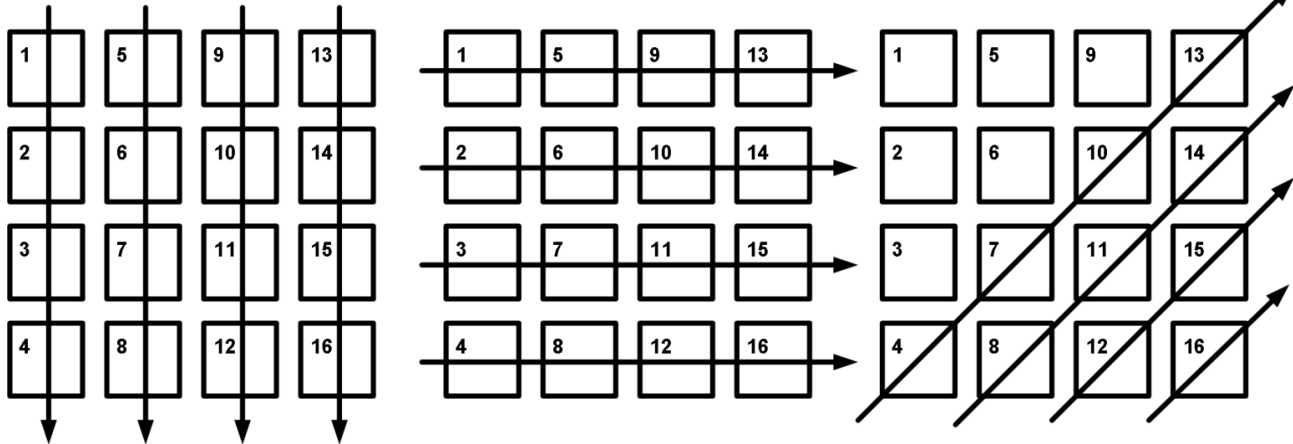


Figure 3: Cell Shading Sequences

The third set of test cases will be to evaluate a random distribution of shade across the array. Each test begins with a set mean irradiance level and the variance from the mean is progressively increased after each test. Once a test is completed, the performance is evaluated and a new value for the mean irradiance is tested. This will mimic the effect of “dappled” light with various intensity values and distributions. For example, if the dappling is light, then the irradiance will be reduced in the range 100% to 90% for a 10% variance range, however if the variance is 50%, then the irradiance will vary across the range 100% down to 50%

Voltage

In this case, the maximum cell power can be seen to be approximately 80W for $1000W/m^2$ of irradiance on the module, and we can vary the irradiance incident onto the panel and there will be an approximately linear relationship between the input and output power in most cases

B. Standard Test Cases

In order to have a level playing field when comparing the different configurations, we have defined several reference test cases to allow a direct comparison between the various alternative techniques. Using our simulation platform we can irradiate any specific cells in the range 0% (completely shaded) to 100% (full sun), and observe the effect on an array.

In the first case of basic testing it is assumed that the cells will be completely shaded and the number of cells to be shaded will be set to 1,2,3,4,...,16 with possible sequences shown in Figure 3. This will not only evaluate the tolerance of an array to the specific case of full shade (i.e. full shadow) but also the effect of a cell failure. These tests are repeated to illustrate the effect of partial shading where we define the shaded irradiance as 10% of the full sun level to mimic the real-world case of at least some light reaching the module.

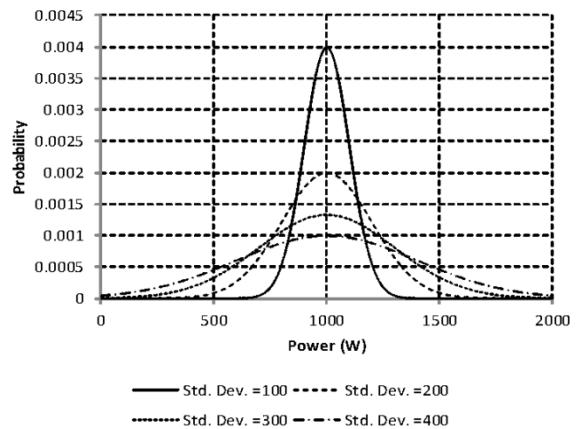


Figure 4: Distribution for different irradiance mean values

C. Standard Test Case 1: Single String of 16 Modules with Bypass Diodes every 4 modules

In this standard test case, the modules are in a single string, with bypass diodes every 4 modules. This is effectively a configuration in single column, with 16 rows in total. The configuration is shown in Figure 5. Each module is numbered from 1 to 16 to make referencing clear and unambiguous.

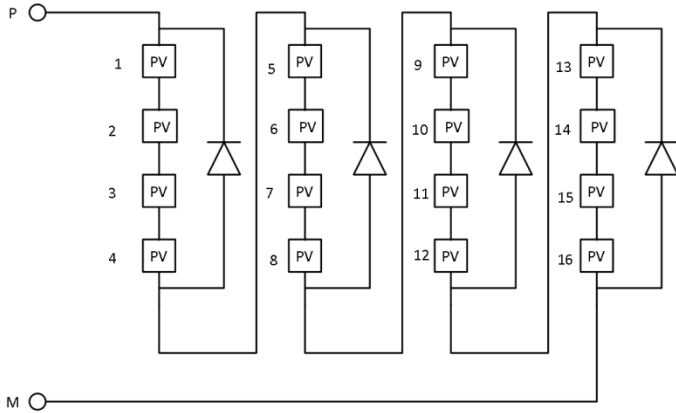


Figure 5: Static 4x4 Reference Array with Bypass Diodes

When this array was tested with a uniform 1000W irradiance on each panel the maximum power point was measured at 1277W, which is almost exactly 16 times the individual module maximum power of 80W. This is the reference point from which all the subsequent power outputs are referenced, as this is the equivalent of each individual module operating at its maximum power point, and the MPPT correctly identifying this point.

If a single module is shaded by 90%, so there is the equivalent of 100W irradiance on a single cell, then the power drops to 911W, which is only 71% of the reference power. The effect of the bypass diodes mean that if the shading occurs on any of the string of 4 modules within a single diode range, then the power will remain the same for 2,3 and 4 cells shaded. If the cell is outside of the bypass diode range, then the result will be to reduce the overall power even further. For example, if module 16 is shaded by 90% and then modules 13, 14 and 15 are also shaded, then the power will drop to 911 W in all cases. If modules 12 and 16 are shaded, then the power will drop to 547W which is only 42.8% of the original reference power. This highlights the poor ability of standard PV modules to cope with partial shading.

If the irradiance is then statistically varied by 25% (in the range from 75% to 100% irradiance, i.e. $875W \pm 12.5\%$), then the impact on the power output can also be calculated. In this case, the mean power output was 1064W, with a standard deviation of 29.75W, and a $\pm 3\sigma$ range of 975W to 1154W. The issue with this type of structure is that the array sections between the bypass diodes are essentially restricted to the performance of the lowest output cell. The results of the statistical analysis also indicate that the impact of a single shaded cell is much worse than a gradual and varied drop across the entire array. This sensitivity to single cell failure or shading is an important reason why new techniques were required to cope with these issues in a better way.

III. IEQUALIZED –DPVA

A. Introduction

In order to cope better with partial shading conditions a new concept called Irradiance Equalization (IE) was proposed in [12]. This type of DPVA is a direct attempt to reduce the current limiting effect caused by partial shading of the array and was the first time that a sophisticated switching method had been used to mitigate issues with irradiance mismatching. By intelligently connecting PV modules through switches into a total cross tied configuration (TCT), the system is able to balance the effective irradiance across each tier in the TCT structure. This ability to reconfigure the modules means that the DPVA can potentially produce many times more power than a static equivalent under undesirable irradiance conditions. Figure 6 shows how the layout of the TCT architecture, where columns of cells or modules correspond to voltage output and rows of cells will provide current. For example, unlike the static array, where the strings of cells were defined explicitly, in the TCT array, the cells will align automatically. For example, in the previous case, where module 16 was shaded, the result would be that cells 13,14 and 15 would be effectively removed from the system, however the result in the TCT is that this effect is reduced.

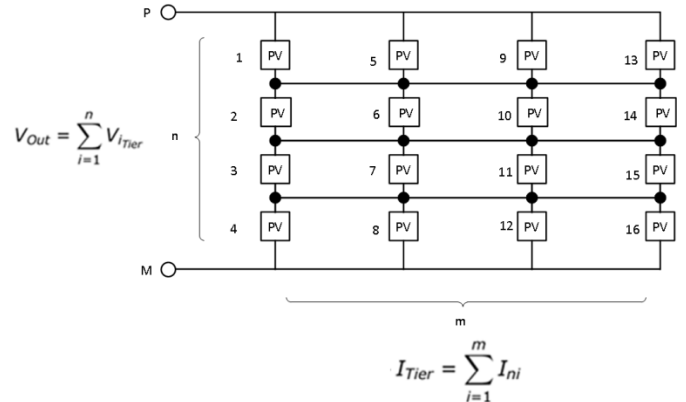


Figure 6: Total Cross Tied configuration

B. TCT Arrays and Irradiance Equalization

Parallel connected solar cell topologies exhibit an extraordinary resilience to power limitation caused by partial shading [21] and as a result the current produced by each ‘tier’ will be the sum of the currents from all cells within a row. The voltage produced by the string of tiers will be the sum of the voltages of each tier. As solar cells are primarily current sources, the voltage they produce is logarithmically proportional to the currents flowing internally, and consequently it will remain relatively steady for output currents below the maximum power point, I_{MPP} . From this it can be said that the voltage of the array will maintain a predictable level if all tiers are operating below I_{MPP} .

Irradiance Equalization is the process of swapping the cells from one tier to another so that the total irradiance (and therefore current producing ability) at each tier is almost equal. For optimal performance, each tier should contain an

equal fraction of the total insolation falling across the array surface. This ‘optimal irradiance’ value is simply found by adding up all of the irradiances and dividing by the number of tiers. Once an equalization has been done, a simple way to evaluate the array’s choice of configuration is to subtract the weakest performing tier from the best performing tier, where the answers closest to zero indicate good equalization, a second way is to define the power producing abilities as a percentage referenced to a perfectly balanced array as described in Equation (2).

$$Efficiency = \frac{100}{optimal} \times Tier_{Lowest} \quad (2)$$

C. The limitation of “Configurations of Interest – COI”

Using the irradiance equalization approach, it is possible for a 4x4 array to have 20^{12} different possible permutations. Due to the interconnections of the TCT configuration, swapping tiers around has no effect and neither does swapping cells around within a tier. This characteristic has been highlighted in [12] and the number of unique arrangements that produce different output characteristics can be calculated by Equation 3 and are referred to as ‘the configurations of interest’.

$$COI = \frac{(m \times n)!}{m! \times (n!)^m} \quad (3)$$

Even with this reduced number of possible arrangements, a 4x4 array has around 8^6 configurations of interest (262,144) and a 5x5 array has 5^{12} configurations (244,140,625). The current method for defining the optimal configuration is to identify the irradiance profile of the cells, calculate the averaging ability of each configuration of interest and then pick the best one. As this requires an impractical number of calculations, large arrays cannot be effectively controlled by this algorithm. Section IV.A discusses a potential algorithm that can quickly identify a configuration of acceptable equalization.

D. Irradiance Profiling

The irradiance profile is a virtual map containing information about a cell’s physical location and the irradiance across its surface. It is required in order to figure out the optimal configuration and then derive how to correctly control the switch matrix. There are several methods for estimating a cell’s irradiance profile from- IV measurements. Equation (4)

defines the irradiance using IV samples and a proportionality coefficient whereas Equation (5) estimates the photo generated current of a cell based on V_{oc} (the open circuit voltage).

$$I_{rr} = \alpha \cdot [I_i + I_o \cdot (e^{\frac{V_i}{nV_t}} - 1)] \quad (4)$$

$$I_i = I_o \cdot \left(e^{\frac{V_t}{nV_t}} - 1 \right) + \frac{V_{oc}}{R_{shunt}} \quad (5)$$

A novel technique that requires no extra sensors and that can build a very accurate profile based on the value of each cell I_{MPP} is described in section IV.D

E. Effectively Shaded Columns

The array’s ability to equalize depends on the number of shaded cells and the severity of the shading. As the previous IEQ-DPVA must maintain N tiers for all configurations, there are some scenarios where the current is being restricted and reconfiguring will not cause this to change. If the TCT configuration in Figure 6 is considered under partial shading conditions, where cell 16 is shaded by 90% (i.e. only 10% irradiance), we would expect the overall array to provide more than 94% of the rated power, however in practice the actual power drops to around 88%

As can be seen in Figure 7, the result is that even though only cell 16 is shaded, the effect on the TCT array is to effectively shade the remainder of the column as if they were in partial shade. Switching the shaded cell around will not improve power extraction and the amount of power being lost is equal to sum of the unused power in the unaffected tiers. Section IV.C suggests a method that can improve power extraction by reducing the number of cells within ‘effectively shaded columns’. In

Figure 7(b), cells 13, 14 and 15 can be seen to effectively be partially shaded by cell 16, resulting in a further 6% drop in addition to the 6% drop one would expect from a single shaded cell in isolation. In the figures in this paper, where a PV cell is shown with a white background, this indicates no shading, a solid black background indicates the cell has been actively shaded (10% irradiance for the purposes of this work) and the light grey shaded background indicates cells where although a cell is not actively being shaded, there is some effect from neighboring shaded cells.

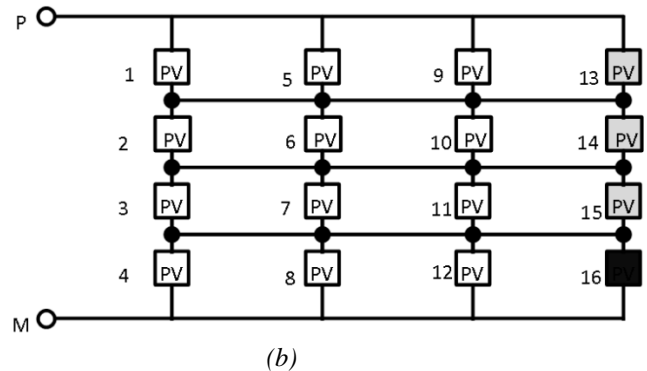
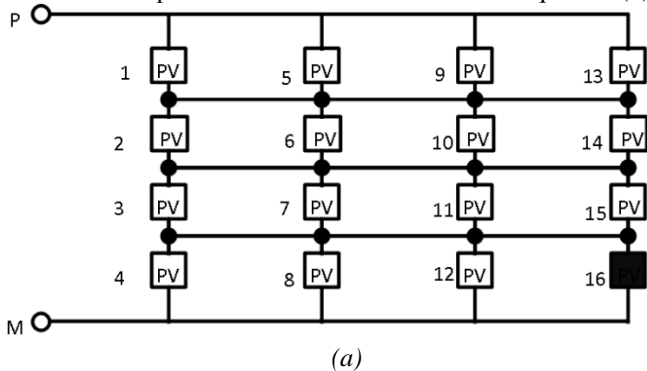


Figure 7: Effective column shading

This situation gives rise to an asymmetry between multiple shadings within a column and multiple shadings

within a tier. For every cell shaded within a tier, another whole column becomes effectively shaded whereas additional shaded cells within a column have no effect on power production. In the column shading test, the cells were shaded in the column sequence of cells 16,15,14,13,...,1. In the row shading test, the cells were shaded in the sequence 16,12,8,4,15,...,1. In all cases the cells were shaded by 90%.

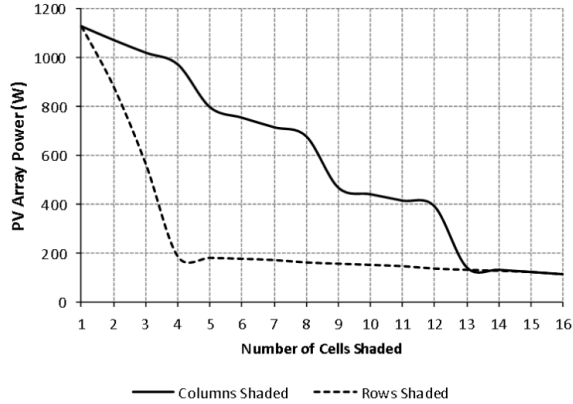


Figure 8: Row-Column loss comparison for 4x4 TCT array

This illustrates one of the key problems with the TCT structure where the shading pattern can have a dramatic effect on the performance of the array as a whole. For example,

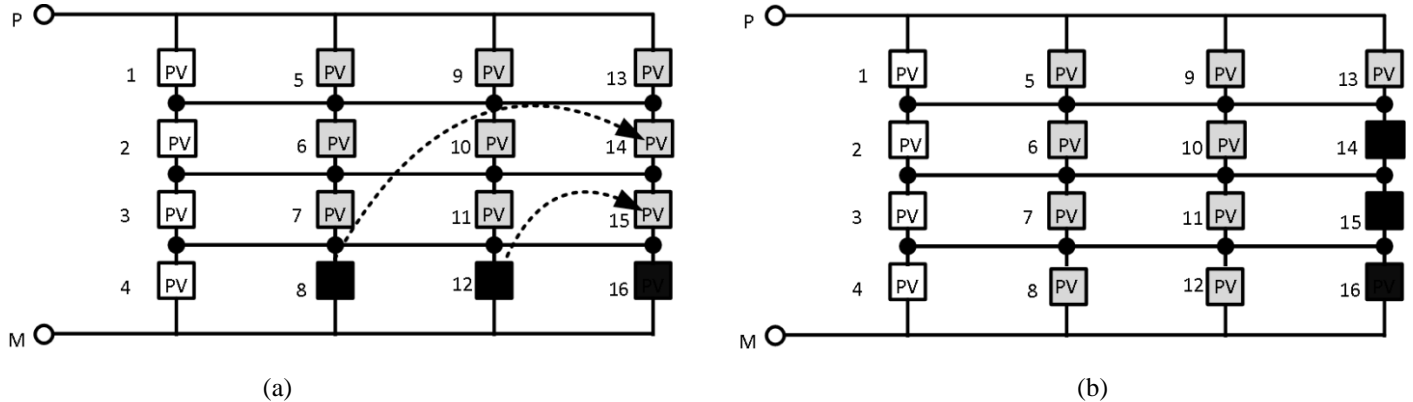


Figure 9: Relocation of shaded cells into effectively shaded columns

IV. OPTIMIZING THE IEQ-DPVA

A. Improving the search time

One of the biggest limitations of the system described in [12] is the time it takes for the controller to execute the optimization algorithm. As has been discussed previously in this paper, the possible permutations in even a small 4x4 array mean that this architecture is not able to be optimized in real time, and so a quicker more efficient approach is required. The algorithm proposed in this paper is an iterative and hierarchical sorting algorithm that is designed to establish near optimum configuration within a small number of iterations. As with the system discussed in [12], the cells are profiled. The resulting data fields obtained are then arranged in descending order and converted to a matrix of the desired size to match the physical array. Next, all even rows are flipped

left to right and added to the preceding odd row. The best of the odd rows have now been paired with the worst of the even rows and the result is an average. These ‘averaged rows’ are then resorted; the even rows are once again flipped and added to the odd rows. The averaged rows have now undergone a second averaging. The algorithm continues to reorganize, flip and add until all rows have been included. If there is ever an odd number of rows (for values greater than two), a padding row of zeros can be added. The algorithm continues until final number of rows is one. Obviously the algorithm requires the number of rows to be a power of two, however an extra rows of zeros can be added to compute the required configuration if the array is not intrinsically a power of two in size. By following the same grouping patterns with the cell’s physical locations, the control signals for the switch matrix can be obtained.

consider the row shading situation where only 4 cells are shaded (16,12,8 and 4) however the resulting power output drops to only 14.6% of the total available power, even though 75% of the cells are still unshaded.

If the array is dynamic, any shaded cells within a tier can be relocated to occupy a position in an effectively shaded column, thus reducing the number of effectively shaded columns. The simplest optimization from this point of view is to have an array where the number of tiers is greater than the number of cell within a tier. This way, more shaded cells can be relocated in the same ‘column space’ and the chance of overflowing into a new column is less likely.

As we can see from the simple relocation of cells example in Figure 9, intelligent adjustment of the tiers can result in significant improvements in overall power output under shaded conditions. In this simple example, if cells 16,12 and 8 are shaded by 90%, then the output power will drop to 44% of the unshaded array. If these cells were relocated using a dynamic switching matrix into positions 16,15 and 14, then the resulting power would be 80% of the unshaded power, which is obviously a significant improvement. The next section will discuss how this feature can be used for optimization.

The algorithm can be expressed as follows:

Algorithm 1: BestWorst Sorting Algorithm

```

Algorithm: BestWorst
  While the number of rows > 1
    Sort the matrix of cell powers in
    numerical order highest to lowest
    Flip the even rows from left to
    right (lowest value to highest value)
    Add each pair of adjacent odd and
    even rows together

```

If a simple example is used to explain this basic idea, the concept becomes clearer. Consider our case of a 4x4 matrix of cells or modules generating different power outputs due to shading and other differences. The power values range from a maximum of 32W down to a minimum of 7W as shown in Figure 10. The algorithm then follows the steps of flipping rows, adding and then resorting until only one row is left with the four distinct power values of 80W, 82W, 82W and 82W. This gives an average power in each row element (which corresponds to a sorted column) of 20W, 20.5W, 20.5W and 20.5W respectively and if the actual average of the raw data is calculated the absolute average is 20.375W. The errors in each case are therefore 0.375W and 0.125W which are less than 2%. The number of iterations of the algorithm is clearly obtained from the order of the matrix, so for a 4x4 matrix, there will be two iterations, 8x8 there will be three and so on. This means the algorithm works in the favour of the system designer for larger systems, rather than against, as is the case for the COI calculation approach.

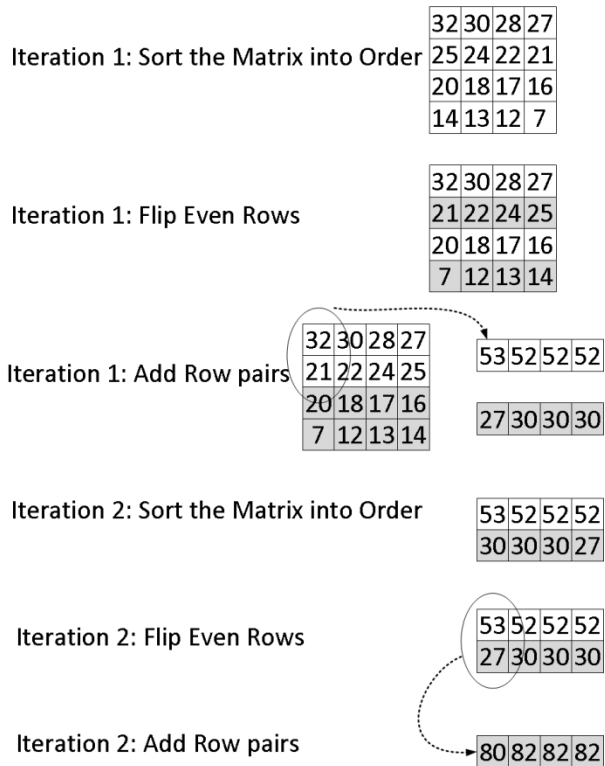


Figure 10: Example algorithm routine

This method is not guaranteed to find the global

maximum configuration, but it will produce a configuration that is within an acceptable margin from the optimum. It takes very little time to execute and the calculation time is almost unaffected by increasing the size of the array. One of the significant advantages of this approach is the simplicity of computation.

B. Repetitive Switch Networks

It is possible to reduce the complexity of the switch network by creating a DPVA that can only produce configurations of interest (COI), as discussed previously in this paper. While this causes a minor reduction in switch count, it also creates a non-repetitive switch structure. This is acceptable when building the switch matrix from discrete components, but in future commercial systems it is anticipated that the switching circuitry will be integrated within a module. Non repetitive structures are therefore inconvenient from this aspect. Another reason why a repetitive switch structure is beneficial is the array becomes fully dynamic and all possible configurations are available for use. This has two ramifications. Firstly, the array is able to resize its dimensions which can improve power extraction (discussed in section IV.C), and it also allows for 'sense configurations' to be applied (section IV.D).

To create a fully dynamic IEq-DPVA, either the DC busses must have interconnectivity via extra switches or the switches connecting the busses to the cell nodes must have the ability to be operated independently. Figure 11 shows a simplified system where the flexibility of the switch matrix is determined by how many possible common connections are available in the module architecture.

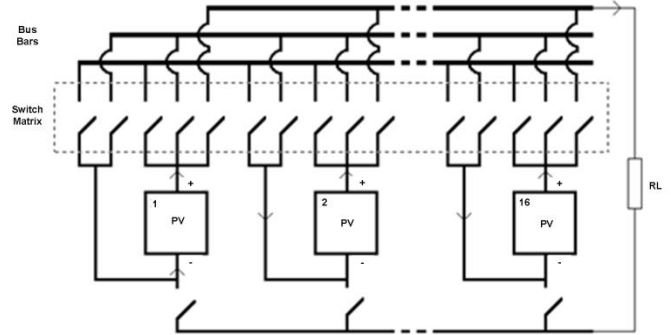


Figure 11: Switch Structure for fully dynamic IEq-DPVA

C. Flexible Array Sizing

An IEq-DPVA which can alter its matrix dimensions will be able to produce better equalization over a wider range of scenarios because some effective shading conditions can be nullified. There exist two options when considering adjustable array sizing and it should be noted at this point that this is not the same as re-configuring. Firstly, 'exact row sizing' is where the dimensions can change in such a way that all tiers maintain the same number of cells. This is the most convenient method of resizing and its implementation is the simplest. A static TCT array can be made into a simple FC-DPVA by implementing exact row resizing and the hardware required is extremely simple. The resulting resized 2x8 TCT array based on the original 4x4 TCT shown in Figure 6 is shown in Figure 12.

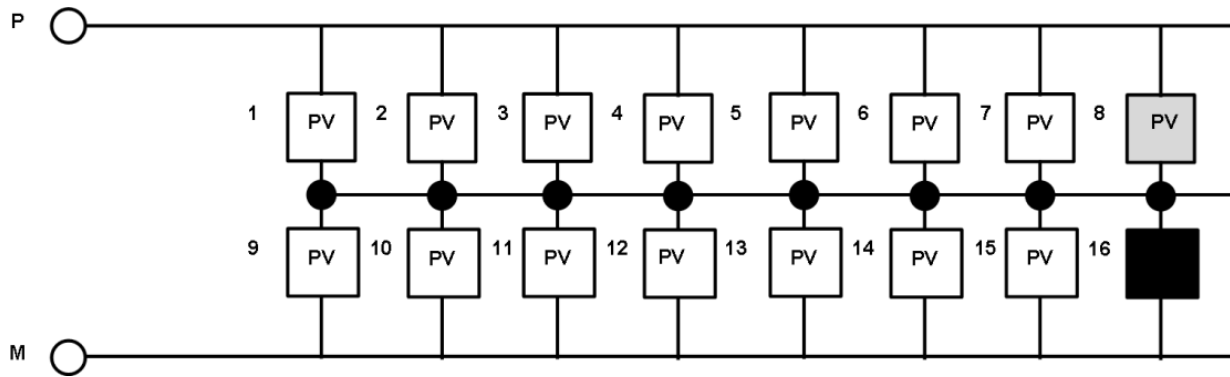


Figure 12: Exact row resizing

By comparing Figure 7(a) and Figure 12, it can be seen that by having the ability to turn a 4x4 configuration into a 2x8 results in effectively two extra cells producing extractable power. The resulting power will increase for the whole module compared to a 4x4 TCT array for a single shaded cell from 88.4% to 92.8% and it can be seen that the architecture will be intrinsically more tolerant of shading as the cells are connected in shorter strings.

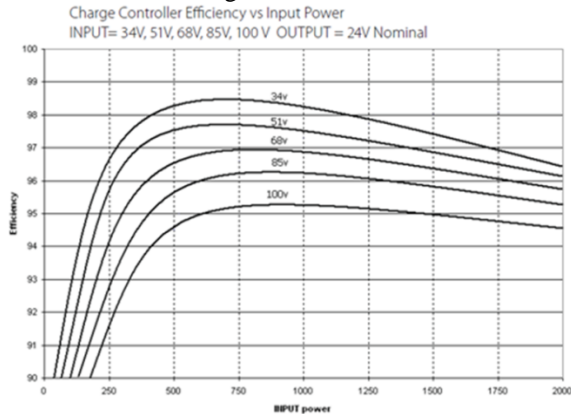


Figure 13: Typical MPPT performance

The voltage will have halved as the configuration changes but as this is a controlled situation, any following power conditioning will know in advance. Many MPPTs accept a wide range of input voltages (typically 12 - 96V [22]) and as long as this range of operation is maintained this should present no practical implementation issues. Figure 13 shows that even for a very wide range of voltage input and power requirements, the overall efficiency of an MPPT is more than 90% in almost every case.

The second way to adjust the array size is to have 'arbitrary row sizes' and this option is an inherent feature of the adaptive bank dynamic photovoltaic array (Ab-DPVA) presented in [14-16], which is a sub-class of the IEq-DPVA. This resizing strategy requires a more complicated sorting algorithm than the simple algorithm presented in this paper, however the principle would allow the array to become fully adjustable. By implementing a repetitive switch network, both resizing strategies become available to the PV systems designer.

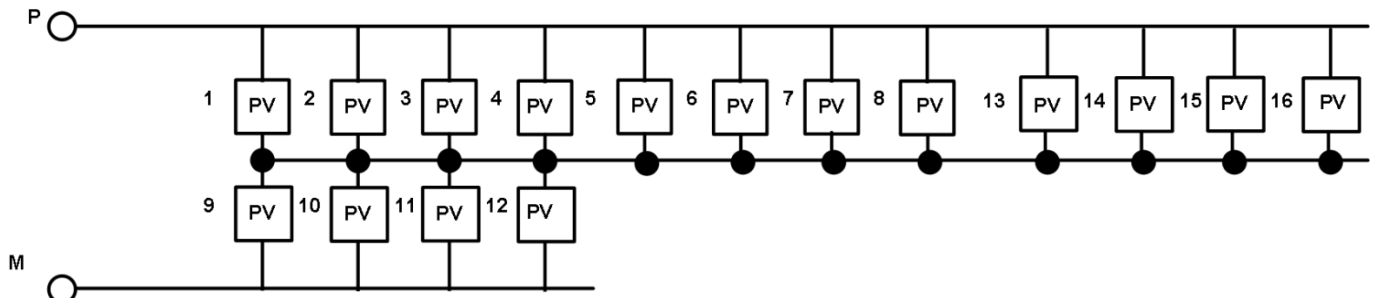


Figure 14: Arbitrary row resizing

D. Sense Configurations

With any advanced DVPA system, it is essential to be able to monitor the status of an individual cell or module. The sense configuration is the process of arranging the entire array so that information about a single cell or module can be gathered. It requires the array to momentarily stop delivering power to the load and begin being loaded by a controlled current sink. The purpose is to collect a precise ' I_{MPP} profile' without the need for estimations while reducing the number of current sensors required to one. In simulated tests the irradiance estimation process was shown to have a maximum

relative error rate of 4.4%. This value could rise significantly in a real system, and accuracy is likely to fall according to increasing array size and age, and therefore it is desirable if possible to maintain up to date characterization information for all the cells across the system to establish optimum operating conditions.

The technique will isolate a single cell from the array by making it operate alone in a tier which is stacked upon the rest of the array. The 'test cell's' voltage will be monitored as the operating current is gradually increased. When the monitored cells voltage reaches the temperature compensated maximum power point (MPP) voltage V_{MPP} , the cell is operating at the

MPP and its current producing capabilities are now known. The process is then repeated for all cells and an accurate profile is created. This is a more precise way of profiling the cells as it is based on real measurements and it directly identifies the MPP of cell. Furthermore, any losses or device mismatches within the array will have been accounted for by the measurement, whereas this may not be the case when profiling is achieved by estimation alone. This general profiling approach has been described previously [23], however we believe that the flexibility of the fully dynamic configurable switch architecture in this paper leads to a much simpler and straightforward mechanism for the accurate profiling of individual cells on demand, and in situ, which also offers the possibility of calibration and also remote testing while the array is in service.

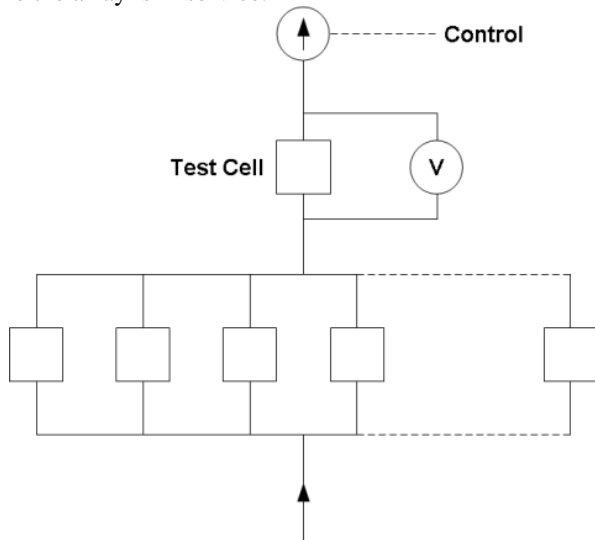


Figure 15: Sense configuration identifying I_{MAX}

V. RESULTS

A. Introduction

A DVPA system simulation platform has been developed using MATLAB ® and SABER ® to verify the proposed algorithm functionality and demonstrate the benefit of employing a resizing strategy. Detailed models were implemented in the Saber simulator to calculate the detailed circuit level behavior and the Matlab model was used to evaluate multiple switch configuration options. In addition to the results presented previously in this paper, we have also simulated an optimally configured 16 cell IEq-DPVA which can be perform exact row resizing such that the standard 4x4 can become a 2x8 matrix. Two test scenarios are presented, one with a randomly distributed irradiance and the other with a defined shading profile.

B. Random Distribution

The simulator requires the mean irradiance value (μ) and the standard deviation (σ) to create randomly selected normal distribution of irradiances (16 in our case). It will then generate the irradiance profile and the algorithm will perform equalization on both 4x4 and 2x8 sized arrays. This process is repeated 1000 times as to find the arrays average equalization capability under each specific distribution condition.

A configurations ability to maximize power is measured as a percentage relative to the mathematical optimal. That is, 100% efficiency occurs when all tiers produce exactly the same power. The results are shown in Table 1, and indicate that the resizing the array provides improvements, with the relative improvement becoming increasingly better for lower irradiance and widely distributed conditions. This indicates the potential for this in highly shaded (urban) conditions. The mean irradiance value is defined in terms of the full power (unshaded) conditions, therefore 100% is full sun and 0% would be fully shaded. The variance is defined in terms of the variation in % from the mean value. Finally, the outputs for the 4x4 and 2x8 arrays are defined in terms of the average power output percentage with reference to the ideal case.

Mean Irradiance (%)	Variance (%)	4x4Array (%)	2x8Array (%)
80	10	98.6	99.5
	20	97.3	99
	30	96	98.6
	40	95.1	98.3
	50	94.1	97.9
60	10	98.1	99.3
	20	96.3	98.7
	30	95.2	98.3
	40	93.7	97.9
	50	92.93	97.5
40	10	97.12	99
	20	95.2	98.3
	30	92.8	97.7
	40	92.3	97.3
	50	91.5	97.1

Table 1: Average performance of sized

IEq-DPVA's under distributed irradiance profiles

These results also indicate that a random variation in irradiance will be compensated for better with a higher variance, which shows that the steeper the changes in irradiance between different cells, the better the reconfiguration will become. As the average irradiance drops from 80% to 40% of full power, for higher levels of variance, the improvement increases from ~4% to ~6%. This is perhaps not unexpected, as with a relatively small array and large granularity (only 16 cells), there will be limited benefit in cell swapping if the irradiance is almost the same.

C. Selected Irradiance profiling

In contrast with the random variation of irradiance, another realistic test case is where the irradiance is “stepped” across specific cells, to model the effect of shading. The test undertaken in this section will concentrate on known patterns of shading across the array. This sort of ‘linear abrupt shading’ is to be expected if the array is to operate within an urban areas. A shaded cell within a fully insolated environment will produce around 10%-30% of nominal power from defused light and albedo glare. Taking the two test cases defined for a

4x4 TCT configuration as shown in Figure 6, the individual cells to be shaded will be 16, 15, 14 and 13 respectively and considering the 2x8 TCT shown in Figure 12, the individual cells to be shaded will be 16,8,15 and 7 respectively.

Shade Irradiance (%)	Number of shaded cells	4x4Array (%)	2x8Array (%)
50	One	90.3	96.7
	Two	93.3	100
	Three	96.5	96.5
	Four	100	100
25	One	85.2	95
	Two	89.6	100
	Three	94.5	94.5
	Four	100	100

Table 2: Performance of sized IEq-DPVA's under abrupt shading profiles

The results of the more abrupt shading profiles indicate that efficiency improvements can result of more than 10% when the array is configured in even these two simple ways.

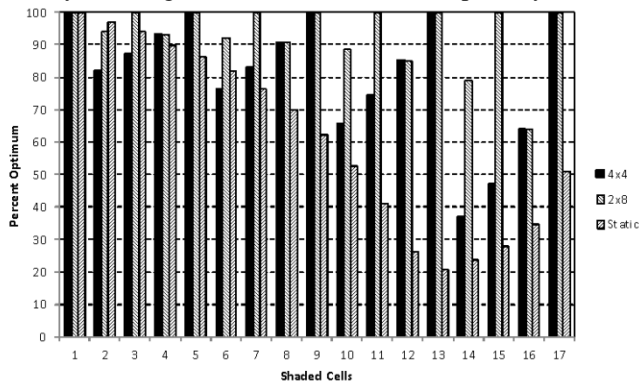


Figure 16: Relationship between power output and shaded cell number

D. Processing Speed

Executing the algorithm on a desktop computer running MATLAB, it takes 300ns of CPU time to calculate the arrangement of a 16 cell array. There will be almost no increase in time for larger arrays as the sorting procedure is very simple, and as-discussed previously in this paper, does not increase linearly with the scale of the array. It is appreciated that this time delay would raise when implemented on a controller running embedded software, but the reactance of the device will still be real time. As the algorithm is based on simple comparisons and swapping, the calculation time will be significantly lower than a second for typical arrays. The reported data acquisition and reconfiguration time as reported in [12] for a 6 cell array using the configurations of interest (COI) computation algorithm takes 200ms. This array has only 15 COI and therefore moving to a 4x4 array with 2,627,625 COI would take 9.7 hours to find the optimum. Clearly, we can infer that for practical situations this will be too long to be useful.

One of the useful aspects of the simple optimization algorithm presented is that the only calculation required is a simple

comparison, and then a swap is decided upon. This means that complex signal processing is not required, and the resulting circuitry and programming can be extremely compact, efficient and simple.

VI. CONCLUSIONS

This research has identified several opportunities for further optimizing an irradiance equalization dynamic photovoltaic array. The use of dynamic arrays has yet to become main-stream but with the increasing need to install PV generators within urban environments, it is possible that reconfigurable arrays will gain preference over static bypassed arrays. These results indicate that with even very simple dynamic PV arrays, efficiency improvements of 10% are achievable over a conventional static array, which can reduce the return on investment by years in a real installation. The potential for smaller granularity systems is even better, with a resulting more flexible and efficient system.

The algorithm presented is designed to be compact and efficient, and can be used to obtain a usable configuration for the array with a minimum of associated circuitry. By considering individual tiers within the array, the resulting configuration will average to near optimum and convert a considerable amount more power than a standard bypassed array under unfavorable conditions. Even when only considering the two simple test cases presented, the number of possible configurations is still so large that calculating every permutation is not feasible for a real time system, so using a simple algorithm to converge to an optimal solution is preferable.

In addition, a simple profiling technique that utilizes less hardware to accurately identify the maximum power point of all cells within the array has been discussed. These sense configurations remove the need for multiple current sensors and the ambiguities associated with the characteristics of individual cells do not cause profiling error rates to rise.

The resizing procedure is a simple way to avoid losses with effective shading as experienced with any TCT connected array. Static TCT arrays can easily be made to perform simple 'exact row' resizing at minimal cost, while fully dynamic arrays can utilize 'arbitrary row sizes' which makes the device extremely flexible. The number of power delivery switches used to create a fully dynamic array will hardly increase relative to existing IEq-DPVA switch topologies. As these extra switches are just repetitions of the existing networks, the extra control hardware can also be the same.

In order for an advanced DPVA system to function optimally, it will have to communicate its operations with the subsequent MPPT power controllers. This is not currently a commercial option, but as DPVA platforms gain preference, the next generation of inverters or MPPT may need to be designed with reconfigurable arrays in mind.

REFERENCES

- [1] M.A. Green, 'The Path to 25% Silicon Solar Cell Efficiency: History of Silicon Cell Evolution' *Progress in photovoltaic: research and applications*, 2009, pp183-189

- [2] B.Stuart (March ,2011) , ‘2010 PV market growth strong’ [Online]. Available: <http://www.pv-magazine.com/news>,
- [3]W. Schockley and H.J. Quiesser, “Detailed Balance Limit of Efficiency of p-n Junction Solar Cells”, *Journal of Applied Physics*, Vol. 32, pp. 510-519, 1961
- [4] D.M. Bagnall and S.A. Boden, “Photovoltaic Energy Harvesting”, 2010
- [5] A. Einstein, “Concerning an heuristic point of view towards the emission and transformation of light”, *American Journal of Physics*, Vol. 33, No. 5
- [6] Acciari, G.; Graci, D.; La Scala, A.; , “Higher PV Module Efficiency by a Novel CBS Bypass,”*IEEE Transactions onPower Electronics* , vol.26, no.5, pp.1333-1336, May 2011
- [7] R. Giral, C.A. Ramos-Paja, D. Gonzalez, J. Calvente, A. Cid-Pastor, L. Martinez-Salamero, “Minimizing the effects of shadowing in a PV module by means of active voltage sharing,”*Industrial Technology (ICIT), 2010 IEEE International Conference on* , vol., no., pp.943-948, 14-17 March 2010
- [8]Y. Nimni andD. Shmilovitz, “A returned energy architecture for improved photovoltaic systems efficiency,”*Circuits and Systems (ISCAS), Proceedings of 2010 IEEE International Symposium on* , vol., no., pp.2191-2194, May 30 2010-June 2 2010
- [9] Z.M Salamehand and F. Dagher, “The effect of electrical array reconfiguration on the performance of a PV-powered volumetric water pump,”*IEEE Transactions onEnergy Conversion*, vol.5, no.4, pp.653-658, Dec 1990
- [10] Y. Auttawaitkul, B. Pungsiri, K. Chammongthai, and M. Okuda, “A method of appropriate electrical array reconfiguration management for photovoltaic powered car,”*IEEE Asia-Pacific Conference on Circuits and Systems*, 1998, pp.201-204, 24-27 Nov 1998
- [11] R. Candela, V. Di Dio, E. Riva Sanseverino and P. Romano, “Reconfiguration Techniques of Partial Shaded PV Systems for the Maximization of Electrical Energy Production,”*Clean Electrical Power, 2007. ICCEP '07. International Conference on* , vol., no., pp.716-719, 21-23 May 2007
- [12] G. Velasco, J.J. Negroni, F. Guinjoan, R. Pique, “Irradiance equalization method for output power optimization in plant oriented grid-connected PV generators,”*European Conference on Power Electronics and Applications*, 2005, p10
- [13] G. Velasco-Quesada, F. Guinjoan-Gispert, R. Pique-Lopez, M. Roman-Lumbreras, A. Conesa-Roca, “Electrical PV Array Reconfiguration Strategy for Energy Extraction Improvement in Grid-Connected PV Systems,”*IEEE Transactions on Industrial Electronics*, vol.56, no.11, pp.4319-4331, Nov. 2009
- [14] D. Nguyen and B. Lehman, “An Adaptive Solar Photovoltaic Array Using Model-Based Reconfiguration Algorithm.”, *IEEE Transactions on Industrial Electronics* , vol.55, no.7, pp.2644-2654, July 2008
- [15] D. Nguyen and B. Lehman, “A reconfigurable solar photovoltaic array under shadow conditions,”*Applied Power Electronics Conference and Exposition, 2008. APEC 2008. Twenty-Third Annual IEEE* , vol., no., pp.980-986, 24-28
- [16] Z. Cheng, Z. Pang, Y. Liu and P. Xue; , “An adaptive solar photovoltaic array reconfiguration method based on fuzzy control,” *Intelligent Control and Automation (WCICA), 2010 8th World Congress on* , vol., no., pp.176-181, 7-9 July 2010
- [17] L.A.R. Tria, M.T. Escoto, C.M.F. Odulio, “Photovoltaic array reconfiguration for maximum power transfer,” *TENCON 2009 - 2009 IEEE Region 10 Conference* , vol., no., pp.1-6, 23-26 Jan. 2009
- [18] M.A. Chaaban, M. Alahmad, J. Neal, J. Shi, C. Berryman, Y. Cho, S. Lau, H.Li, A.Schwer, Z. Shen, J. Stansbury, T. Zhang, “Adaptive photovoltaic system,”*IECON 2010 - 36th Annual Conference on IEEE Industrial Electronics*, vol., no., pp.3192-3197, 7-10 Nov. 2010
- [19] B. Patnaik, P. Sharma, E. Trimurthulu, S. Duttagupta, V. Agarwal, “Reconfiguration strategy for optimization of solar photovoltaic array under non-uniform illumination conditions,”*Photovoltaic Specialists Conference (PVSC), 2011 37th IEEE* , vol., no., pp.001859-001864, 19-24 June 2011
- [20] M. Alahmad, M.A. Chaaban, S.K. Lau; , “An Adaptive photovoltaic-inverter topology,”*Innovative Smart Grid Technologies (ISGT), 2011 IEEE PES* , vol., no., pp.1-7, 17-19 Jan. 2011
- [21] L. Gao, R.A. Dougal, S. Liu and A.P. Iotova, “Parallel-Connected Solar PV System to Address Partial and Rapidly Fluctuating Shadow Conditions,”*Industrial Electronics, IEEE Transactions on* , vol.56, no.5, pp.1548-1556, May 2009
- [22] Flexmax 80, Outback Inc., Datasheet, http://www.outbackpower.com/pdf/manuals/flexmax_80.pdf
- [23] M. Bodur and M. Ermis, “Maximum power point tracking for low power photovoltaic solar panels,”*Proceedings 7th Mediterranean Electrotechnical Conference, 1994*, pp.758-761 vol.2
- [24] Y.H. Ji, D.Y. Jung, J.G. Kim, J.H. Kim, T.W. Lee and C.Y. Won, “A Real Maximum Power PointTracking Method for Mismatching Compensation in PV Array Under Partially Shaded Conditions,” *IEEE Transactions on PowerElectronics*, vol.26, no.4, pp.1001-1009, April 2011
- [25] A.K. Abdelsalam, A. M. Massoud, S. Ahmed, P.N. Enjeti, “High-Performance Adaptive Perturb andObserve MPPT Technique for Photovoltaic-Based Microgrids,” *IEEE Transactions on Power Electronics*, vol.26, no.4, pp.1010-1021, April 2011
- [26] L. Zhang, W.G. Hurley, W.H.Wölfle, “A New Approach to Achieve Maximum Power Point Trackingfor PV System With a Variable Inductor,” *IEEE Transactions on Power Electronics*, vol.26, no.4, pp.1031-1037, April 2011
- [27] B.N. Alajmi, K.H. Ahmed, S.J. Finney, B.W. Williams, “Fuzzy-Logic-Control Approach of aModified Hill-Climbing Method for Maximum Power Point in Microgrid Standalone Photovoltaic System,”*IEEE Transactions on Power Electronics*, vol.26, no.4, pp.1022-1030, April 2011
- [28] L. Zhou, Y. Chen, K.Guo, F.Jia, “New Approach for MPPT Control of Photovoltaic System WithMutative-Scale Dual-Carrier Chaotic Search,” *IEEE Transactions on Power Electronics*, vol.26, no.4, pp.1038-1048, April 2011
- [29] K. Ishaque, Z. Salam, M.Amjad, and S.Mekhilef, “An Improved Particle Swarm Optimization (PSO)–Based MPPT for PV With Reduced Steady-State Oscillation,” *IEEE Transactions on Power Electronics*, vol.27, no.8, pp.3627-3638, Aug. 2012